$\Delta\nu_{dd}$ splitting caused by *direct* magnetic dipole-dipole interactions

$\Delta\nu_{Q}$ quadrupolar splitting

$\Delta\nu_{Q,L}$ quadrupolar splitting of the steady state lamellar phase

ε half bilayer thickness

ζ wandering exponent

η viscosity

θ angle between a vector and $\vec{B}$

θ_{db} angle between the director of an anisotropic phase and the magnetic field

θ_{nb} angle between surfactant layer normal and the magnetic field

θ_{nd} angle between surfactant layer normal and the director of the liquid crystal

θ_{qn} angle between the efg and the normal of a layer which impedes molecular tumbling

κ rigidity modulus

$\bar{\kappa}$ saddle splay modulus

λ *de Broglie* wavelength *or* elongation factor

μ chemical potential

$\vec{\mu}$ magnetic moment of an atomic nucleus

μ_0 permeability of a vacuum $\mu_0 = 4\pi\cdot 10^{-7}\ \mathrm{T^2J^{-1}m^3}$

μ_N nuclear magneton $\mu_N = 5.0507866\cdot 10^{-27}\ \mathrm{JT^{-1}}$

ν frequency

ν_L Larmor frequency

$\nu_{L,0}$ Larmor frequency of nucleus of reference

ν_Q resonance frequency for the transition between energy states modified through nuclear quadrupolar interactions

ν^+, ν^- resonance frequencies of a quadrupolar doublet ($I = 1$ condition)

ρ macroscopic density

$\rho(t)$ autocorrelation function

ρ_s scattering length density

ρ_d scattering length density of a domain consisting of several components

σ shielding constant *or* surface energy *or* invariance of a bilayer

τ relaxation time constant *or* another specified amount of time

τ_c correlation time

τ_l life time

τ_P^{-1}	rate of bilayer contact (indirectly a probability)
φ	volume fraction of the lamellar phase
ϕ_{B+C}	bilayer = membrane volume fraction
ϕ_C	surfactant volume fraction
$\phi_{C,i}$	surfactant volume fraction of the interface
χ	nuclear quadrupole coupling constant
χ_E	Euler-Poincaré characteristic
χ_P	coalescence parameter
ψ	mass fraction of a stated component *or* constant of the *Avrami* equation determining the type of nucleation
ω	angular velocity in rad/s
ω_b	surfactant to oil plus surfactant volume ratio
ω_L	Larmor angular velocity in rad/s

cps	counts per second
efg	electric field gradient
EPM	'equal peak moment', the point in time where the coexisting peaks in the NMR spectrum of an L_3 to L_α transition have the same intensities
FID	free induction decay
KJMA	*Kolmogorov*, *Johnson*, *Mehl* and *Avrami*
MAPA	'mobile, through adsorption partially aligned'
ME	microemulsion
*n*D-	*n* dimensional
NMR	nuclear magnetic resonance
NQR	nuclear quadrupole resonance
r.f.	radiofrequency
SANS	small angel neutron scattering
T-jump	temperature jump
TR-SANS	time resolved SANS

Table of Contents

1. Introduction **1**

1.1 Complex Fluids **1**
1.2 Motivation and Objectives **3**

2. Phase Behaviour **7**

2.1 Binary System H_2O-$C_{12}E_5$ **8**
2.2 Ternary System H_2O - n-decane - $C_{12}E_5$ **9**
2.3. Phase Behaviour Measurements **13**

3. Theoretical Description of Bilayer Characteristics **16**

3.1 Curvature of Amphiphilic Films **16**
3.2 Bending Energy **18**

4. Mechanisms of Passage Formation and Destruction **20**

4.1 Passage Formation **20**
4.2 Passage Destruction **21**

5. Relaxation Kinetics **25**

6. Nucleation **28**

6.1 Classical Nucleation Theory **28**
6.2 The KJMA Model **31**

7. NMR-Spectroscopy **33**

7.1 Basic Principles **34**

7.1.1 Spin Angular Momentum and Magnetic Moment 34
7.1.2 The Influence of a Magnetic Field 36
7.1.3 The Influence of Radiofrequency Radiation 39
7.1.4 Signal Detection, Free Induction Decay (FID) and Lineshape 41
7.1.5 Relaxation and Correlation Time τ_c 45
7.1.6 Magnetic Shielding, Chemical Shift and Equivalent Nuclei 49
7.1.7 Spin-Spin Coupling 51
7.1.8 Quadrupolar Interactions 52
7.1.9 NMR Experiment Time Scale and Chemical Exchange 57

7.2 The NMR Experiments **60**

7.2.1 D_2O, the Probe Molecule 60
7.2.2 The Two-Sites Model 63

7.2.3 Direct Dipole-Dipole Interactions 65
7.2.4 NMR Signal of the Steady State Isotropic L_3-Phase 66
7.2.5 NMR Signal of the Steady State Anisotropic L_α-Phase 67
7.2.6 L_3/L_α Transition Experiments 69

7.2.6.1 Experimental Procedure 69
7.2.6.2 L_3 to L_α Transitions 70
7.2.6.3 L_α to L_3 Transitions 78
7.2.6.4 Additional Experiments 82

7.3 Analysis of the Experimental Findings 85

7.3.1 L_3 to L_α Transitions 85

7.3.1.1 Kinetic Analysis and Re-Evaluation of the Preliminary Experiments 89
7.3.1.2 Kinetic Analysis of the Established Experiments 93
7.3.1.3 Trends in the Development of the L_α-Phase Volume Fraction φ 102
7.3.1.4 General Kinetic Behaviour 107
7.3.1.5 Splitting Development 112
7.3.1.6 Sponge and Lamellar Peak Width Development 116

7.3.2 L_α to L_3 Transitions 119

7.3.2.1 The Two States Model and the McConnell Equation 119
7.3.2.2 Failure of the Two States Model 122
7.3.2.3 Spectra Fitting 122
7.3.2.4. Trends in the Development of the Fitting Parameters 127

7.3.3 Kinetics of the 'Additional Experiments' 132
7.3.4 Experiments Separating Nucleation from Growth 134

7.4 Interpretations of the Experimental Findings 137

7.4.1 The Driving Force of the L_3/L_α Phase Transition 137
7.4.2 Influence of the Magnetic Field 138
7.4.3 Shift of Resonance Frequency 139
7.4.4. Experimental Data vs. Fits and Simulation 140
7.4.5 L_3 to L_α Transitions 141

7.4.5.1 Characteristics of the Nucleation and Growth Mechanism 141
7.4.5.2 Quadrupolar Splitting of the Steady State Lamellar Phase 144
7.4.5.3 Significances of the Quadrupolar Splitting Development 146
The Effects of Initial Nuclei Orientation on Lineshape 147
Splitting Development Comparisons at Varying Amplitude of the T-Jump 148
Diffusion and the Dilution Effect 150
Splitting Development: Comparisons at Varying Concentration 153

7.4.5.4 Development of Peak Width 155
7.4.5.5 The L_3 to L_α Phase Transition Kinetics 156

The Kinetics in the Light of the CNT 157
Kinetics in the Light of the Passage Destruction Mechanism 163

7.4.6 L_α to L_3Transitions 168

7.4.6.1 Characteristics of the Phase Transition Mechanism 168
7.4.6.2 The L_α to L_3 Phase Transition Kinetics 169
7.4.6.3 The Kinetics in Light of the Passage Formation Mechanism 172
7.4.7 The 'Additional Experiments' 176

8. Small Angle Neutron Scattering (SANS) 177

8.1 Fundamentals of Scattering 177
8.2 Geometry of the SANS Experiments 179
8.3 Contrast Variation 181
8.4 Data Processing 183
8.5 The Equilibrium L_3 State 185
8.6 Temperature Jump Experiments 188
8.6.1 The L_3 to L_α Phase Transition 189
8.6.2 The Equilibrium L_α State 196
8.6.3 The L_α to L_3 Phase Transition 198
8.7 Interpretations of the Experimental Findings 202
8.7.1 The Sponge and Lamellar Steady States 202
8.7.2 TR-SANS, the Kinetic Investigations 204

9. Summary 213

10. Appendices 218

11. Tables 240

12. References 253

1. Introduction

1.1 Complex Fluids

An elemental principle of chemistry concerned with the solution of a component (the solute) in a solvent is generally known even by non-scientists through the simple rule of thumb 'like dissolves like'. This rule refers of course to the polarity of a substance, differentiating simply between polar and nonpolar components, which are regularly termed as being hydrophilic and lipophilic respectively. The latter expressions stem from Greek and are associated with the two main classes of biological solvents, i.e. water on one hand and fats or oils on the other.

Both living nature and modern industry are faced with the problem of intermingling components of the two opposite groups on microscopic length scales and thus resort to using amphiphiles, i.e. molecules that contain both a hydrophilic and lipophilic moiety. These molecules necessarily situate themselves between domains of hydrophilic and lipophilic character (i.e. they reside in the *interface*[1,2,3,4]) because of lowest energy considerations, as the components reduce the interfacial tension between the opposing substances. This in turn results in increasing the miscibility of fluids or, in case of a solid surface and a liquid phase, facilitates wetting and spreading. When amphiphiles function in this manner, they are normally denoted as surfactants. The term 'surfactant' is a linguistic blend of '**surf**ace **act**ive **a**ge**nt**'.

When a water (**A**) and an oil (**B**) component form a macroscopically homogenous mixture due to the presence of a surfactant (**C**) and the input of energy through mechanical perturbation, one speaks of an emulsion. The dispersed phase is present in surfactant coated spherical droplets of the micrometer scale and the internal interface is relatively small. Such mixtures are only kinetically stabilised and degrade over time[4,5,6], i.e. phase separation occurs. If however surfactant concentration is increased the formation of so called microemulsions (ME) becomes feasible. In these mixtures, the required interfacial energy is so extraordinarily low that the present thermal energy suffices to ensure thermodynamic, i.e. indefinite, stability. Thus, microemulsions are nanostructured, thermodynamically stable and macroscopically isotropic homogeneous mixtures of water-oil-surfactant[7,8,9]. Compared with the emulsions, ME have a much larger internal interfacial area and accordingly the structures they exhibit exist on the nanometer scale.

These structures can be surprisingly intricate and can be separated into two general categories, namely discrete aggregates and extended structures. The former include the well-known spherical micelles, but also rod-shaped or disc-like aggregates, while the latter contain extended surfactant films which form structures of various symmetry (e.g. cubic and hexagonal), but also far-reaching tubular networks or simply stacks of sheets. In all of the described cases the surfactant films separate the hydrophilic from the lipophilic domain(s) with a *monolayer* of amphiphilic molecules. It is not surprising that mixtures of this kind are allocated to a general class termed complex fluids, i.e. fluids containing some sort of structure.

Interestingly, complex structures similar to the afore mentioned exist even in the case of simple two component systems, i.e. oil - surfactant and water - surfactant mixtures. That is to say, amphiphilic molecules are not randomly dispersed within their solvent, but rather tend to form a variety of structures through self-assembly, provided that they are present in a critical (but low) concentration. The exact type of present structure is dependant on the existing physical conditions, mainly system composition and temperature. However, in contrast to the three component systems, the surfactant films of two component mixtures are inevitably composed of a *bilayer* of amphiphilic molecules, so that the molecular region of opposite characteristic is isolated from the solvent. The importance of the phenomenon of self-assembly can not be overestimated as life is only possible through compartmentalisation, which is brought about by the existence of biological membranes and amphiphiles in the form of phospholipids are one of their main constituents.

Due to the fluidity of the systems in which they are contained, surfactant bilayers as well as monolayers are highly dynamic in character and it is important to bear this in mind even when a phase and therefore its structures, are in thermodynamic equilibrium. Owing to over half a century of study, equilibrium phase behaviour and the existence of the exhibited structures of water-oil-surfactant systems are by in large understood and accordingly theoretically described[10,11]. Consequently, the focus has shifted to the investigations of phase transitions and specifically their associated kinetics[12,13].

While phase transitions *per se* are a phenomenon that transcends all the natural sciences from astrophysics to zoology[14,15], phase transitions involving membranes/bilayers are mainly a focus of biochemistry and biophysics, as bilayer fusion and fission is an integral part of many cellular processes (e.g. cell division, exocytosis, endocytosis, chemical synapses in neurons, mitochondrial[16] and peroxosimal[17] division). In particular, the investigation of lipid bilayer fusion has received much attention and in that topic especially a proposed mechanism

where an intermediate 'stalk' structure[18,19,20,21] is followed by 'pore formation'[22,23]. However, most of the associated studies are either of a purely theoretical nature or numerical simulations, that is little experimental work has actually been performed and the current state of affairs appears as yet unsatisfactory[24]. Also, biological systems are by their very nature excessively complex and in order to gain underlying understanding of the topic, experiments on simplified model systems are needed. Ternary microemulsions of water, oil and surfactant with their well described bilayer physics can represent such a system.

1.2 Motivation and Objectives

This thesis approaches the subject of amphiphilic bilayer fusion and fission on a most basic level. In essence, it deals with the transition between two bilayer structures of fundamentally different topologies, those of the lamellar or L_α-phase and those of the sponge or L_3-phase (fig. 1.2(1)). These structures are examined in a very dilute system, i.e. the dominating component is water, in resemblance of biological systems. Accordingly, the hydrophilic region of the surfactant molecules faces 'outward', while the hydrophobic region is contained within the bilayer. The L_α-structure consists of stacks of planar, in theory infinite, bilayer sheets and can thus be considered a lyotropic liquid crystalline phase of long-range smectic order. The L_3-phase consist of a single, multiply connected bilayer without seams or edges, which separates two continuous, interwoven water domains that are independent of each other. The bilayer itself can be seen as a network of interconnected 'passages' or 'handles' of somewhat hourglass-like shape (similar to a catenoid). In fact, the morphology of the L_3-phase has been described as a 'melted' cubic phase[25,26,27,28].

From fig. 1.2(1) it is rather obvious that a transition from the L_α to the L_3 phase requires the formation of the mentioned 'handles' or 'passages' and that this inevitably includes bilayer fusion, while the opposite is true in the reverse case. (Formally this can be understood by the fact that the topologies, in the mathematical sense, of the two structures are different, i.e. the Euler-Poincaré characteristic χ_E of an infinite bilayer sheet is zero, while χ_E is negative for the sponge phase[3].) In fact, in the above mentioned bilayer fusion mechanism with intermediate stalk and ultimate formation of a pore, an expanded pore corresponds to just such a passage (fig 1.2(1b)). Although bilayer fusion/fission processes occur by necessity in all cases where there is a change in membrane topology, the chosen transition is particularly advantageous, because the number of passages in an ideal lamellar phase is exactly defined, i.e. there are none. Furthermore, this transition is of additional interest as the isotropic sponge

phase can be considered to ‘crystallise’ when converting to the anisotropic lamellar state, while ‘melting’ occurs in the reverse case (and indeed the phase transitions in question are achieved through an alteration of system temperature). Attaining macroscopic length scale order through controlled crystallisation is an essential part of producing modern materials for functional devices. Hence, basic research concerned with melting and crystallisation processes is always useful.

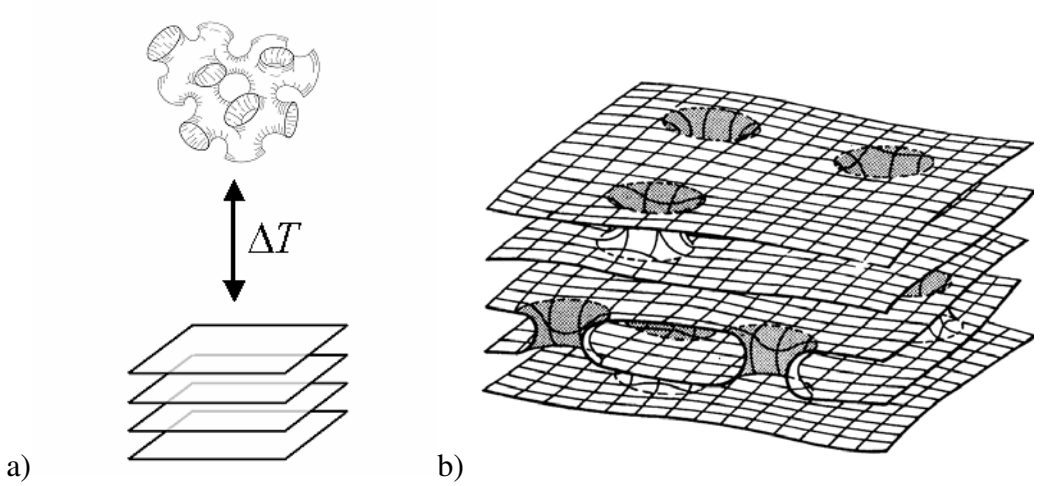

Fig. 1.2(1): a) schematic illustration of the lamellar and sponge phase structures which form after thermally induced phase transitions. The stack of sheets and the continuous passage network represent surfactant bilayers containing the minority oil component. The bilayers themselves are located within bulk water. b) passage formation between lamellae corresponding transition state towards the sponge phase. Concept and figure taken from ref. [29].

All investigations presented in this dissertation were performed on highly dilute microemulsions of the water - *n*-decane - $C_{12}E_5$ system, where $C_{12}E_5$ corresponds to the nonionic surfactant *n*-dodecylpentaoxyethylene. Additionally, the surfactant to oil plus surfactant volume ratio ω_b was kept constant at $\omega_b = 0.45$. Thus, since the water component is excessively dominating and there is respectively little hydrocarbon oil, the membrane structures of the sponge and lamellar phases are still essentially bilayers, even though they are somewhat ‘swollen’ with *n*-decane. The primary reason for the choice of this particular system with its specific ω_b is the fact that it has been intensely studied, i.e. its equilibrium thermodynamic and bilayer elastic properties have been determined. Also, and notably, the dynamics of its L_3-phase have been thoroughly investigated in close cooperation with *Prof. Dr. Olsson* from the Department of Physical Chemistry 1, Lund University, Sweden. This thesis is in effect the result of the continuation of this fruitful cooperation. However, the original selection of the system in question was of course anything but arbitrary.

Firstly, the use of a nonionic surfactant avoids complications with long-range electrostatic interactions[30]. Secondly, employing *n*-decane ensures that the $C_{12}E_5$ monolayers are simultaneously saturated both with respect to oil and water. This is advantageous for theoretical considerations[31]. Also, since *n*-decane is insoluble in water the ternary system at hand can be modelled as a *pseudo*-binary one. Finally, the L_3 and lamellar phases are situated at temperatures which are better manageable experimentally, that is to say they are located at lower values, when compared to the simpler binary system of H_2O - $C_{12}E_5$.

Although the lamellar and sponge phases have both been the subject of intense study, transitions between them, especially the involved kinetics, have not. Indeed, quite a few studies have focused on sponge to lamellar transitions, but almost all of them resorted to shearing as the means of inducing this transition. In fact, only two studies were found that actually utilised the change of temperature instead[32,33] and only the first of these focused on the transition kinetics. However, this investigation was carried out using purely visual methods, so termed dark-field *macroscopy* and polarisation microscopy. In addition, the lamellar phase developed in the form of multi lamellar vesicles, i.e. not the classical layer structure investigated here. Finally, the focus was on describing a kinetic pathway when observing transitions, where the initial state consisted of two phases (L_α and L_3) or even three phases (L_1, L_α and L_3) in equilibrium.

L_3/L_α transitions have been previously investigated almost exclusively with scattering techniques. However, since the sponge phase is isotropic and the lamellar phase anisotropic the interesting possibility arises to use heavy water and employ deuterium nuclear magnetic resonance (^{2}H-NMR), as the two phase types then lead to different signals. In general, the application of ^{2}H-NMR to notice phase transitions or to aid in the identification of a particular phase due to symmetry considerations is well established[34]. However, it appears that this method was first used in investigating an L_3 to L_α transition by *Fischer et. al.* only recently[35], while the investigation of the reverse process in this way seems not to have been performed at all. In the study in question, a single time constant was determined by simply monitoring signal intensity and fitting a single exponential. However, the transition itself was induced through a chemical reaction associated with an increasing change of system composition and the opportunity to vary system parameters or conduct a more detailed evaluation was passed by. Nevertheless, the ^{2}H-NMR experiments presented in this dissertation are essentially modelled after that exemplary work.

The aim of this thesis is to examine the kinetics of L_3/L_α transitions by employing time resolved ^{2}H-NMR and small angle neutron scattering (TR-SANS). The majority of the experiments are of the former kind and they were all performed at Lund University during two extended stays, while the latter were performed on two different occasions at the D11 instrument of the Institut Laue-Langevin (ILL) in Grenoble, France. Insight into the importance of key parameters is to be gained by altering the size of the temperature jumps ΔT, the bilayer volume fraction ϕ_{B+C}, and sample viscosity η (through the addition of sucrose). Furthermore, the study is intended to acquire knowledge of the actual mechanisms involved in the process of the two phase transitions.

2. Phase Behaviour

As stated in the introduction, the investigations in this thesis involve transitions between lamellar (L_α) phase and sponge (L_3) phase. A typical L_α phase[1,4] consists of flat bilayers, which are layered arrangements of amphiphilic molecules, possessing one-dimensional order and being separated from each other by water layers (see fig. 2(1,*left*)).

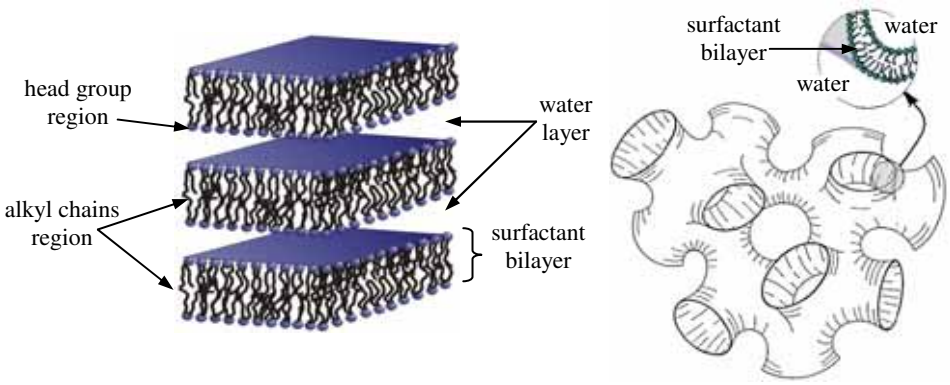

Fig.2(1): structures of extended bilayers: lamellar phase (*left*) and sponge phase (*right*).

Sponge or L_3 phase (see fig. 2(1, *right*)) is an isotropic solution and has up to now only been found in the vicinity of a lamellar phase (L_α)[36,37,38]. Because of its macroscopic appearance, this phase was termed 'anomalous'. It may show strong opalescence and flow birefringence, properties that become increasingly pronounced with dilution. Data resulting from conductivity measurements upon L_3 phase, are quantitatively comparable with what is expected from a bilayer continuous cubic phase, hence the L_3-phase is sometime referred to as a *melted or distorted cubic* phase[25,26,28]. SANS results are consistent with a local bilayer structure. In addition, Freeze Fracture Electron Microscopy (FFEM) investigations upon the topological transformation from dilute lamellar phase to L_3 phase support the idea that there are two main structural differences between L_α phase and L_3 phase: the positional order and the topology[29]. Thus, L_α phase shows long-range smectic order and its bilayers are flat planes, whilst L_3 phase is a liquid-like disordered phase, consisting of 3D multiply connected bilayers and possessing negative monolayer curvature[29,39,40].

2.1 Binary System H_2O - $C_{12}E_5$

Lamellar phase L_α and sponge phase L_3 can be found in the dilute region of the aqueous solutions of surfactants that belong to the well-known class of *n*-alkyl polyoxyethylene (H - $(CH_2)_i$ – $(OCH_2CH_2)_j$ – OH), commonly denoted as C_iE_j . Here *i* informs about the length of the hydrophobic alkyl chain, whilst *j* represents the number of the ethylene oxide groups within the molecule. For the present work the surfactant of choice is $C_{12}E_5$, which when in mixture with water forms a rich variety of phases (see fig. 2.1(2)), with lamellar phase L_α and sponge phase L_3 exhibited at high dilutions.

At very low concentrations the surfactant monomerically dissolves in the water phase. Above a surfactant concentration denoted as *cmc* (critical micelle concentration) the surfactant concentration is sufficient to form microstructures. At low temperatures and low surfactant concentrations these are droplet structures namely micelles which elongate with increasing temperature. At high temperatures the miscibility gap is found.

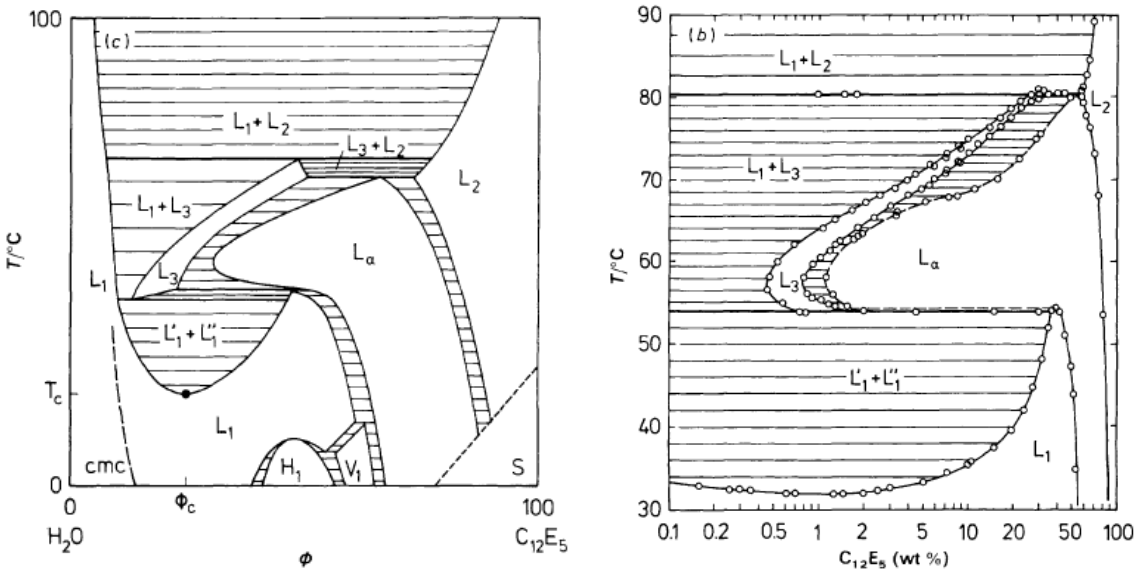

Fig. 2.1(1): a schematic depiction (*left*) and an experimentally determined (*right*) phase diagram of the binary system H_2O-$C_{12}E_5$. Figures taken from ref.[26]

At higher surfactant concentrations, liquid crystalline phases such as hexagonal phase H_1, cubic phase V_1 and lamellar phase L_α are formed. The latter is stable over a wide range of temperature and composition into very dilute regions. In direct vicinity of the L_α phase, towards higher temperatures, separated only by a narrow two-phase coexistence region, the L_3-phase is located. It is evident, that the L_3-phase is stable only over a narrow temperature interval, while extending over a large concentration range. Therefore, one often refers to an

'L_3-channel'. At higher temperatures, the sponge phase is in coexistence with the L_1' phase, a phase similar to the micellar L_1 phase but of higher dilution, i.e. water content.

However, no matter how attractive the simplicity of the above mentioned binary system is, for the study of the L_α / L_3 phase transition there are a few serious limitations from practical, as well as from theoretical perspective (see section 1.2). This limitations can be overcome by introducing a third component, namely an oil (here *n*-decane). This does not only bring the L_α and L_3 phases closer to room temperature, but at the same time ensures the saturation of the $C_{12}E_5$ monolayer in both water and oil.

2.2 Ternary system H_2O - n-decane - $C_{12}E_5$

In general, when describing the phase behaviour of three component systems as function of their composition, it is sensible to resort to using a *Gibbs triangle* spanned by the three components, in order to avoid the complications associated with a three dimensional depiction. Choosing the classical notations from the microemulsions: the water is referred to as the (A) component, the oil as the (B) component and the surfactant as the (C) component. Since the phase behaviour of microemulsion consisting of water (A), hydrocarbon oil (B) and nonionic surfactant(C) is also strongly dependant on temperature, this parameter is added as an ordinate to the triangular base and the result is a phase prism (fig. 2.2(1)). Fortunately, microemulsions of the mentioned type are very insensitive to changes in pressure (an increase of 10 MPa causes a shift of the phase behaviour to higher temperatures by approximately 2-3 K)[41,42], so that for all measurements at the respective ambient condition this parameter is neglected.

The investigations presented in this thesis deal with temperature induced L_3/L_α transitions in the dilute region of the microemulsion-type system H_2O - *n*-decane - $C_{12}E_5$. A schematic phase diagram, inserted into a phase prism, is given in fig. 2.2(1), the area of interest being denoted by a circle.